



UNIVERSITY OF LEEDS

This is a repository copy of *SFR Modelling for Hybrid Power Systems Based on Deep Transfer Learning*.

White Rose Research Online URL for this paper:

<https://eprints.whiterose.ac.uk/197711/>

Version: Accepted Version

Article:

Zhang, J, Wang, Y, Li, H et al. (4 more authors) (2024) SFR Modelling for Hybrid Power Systems Based on Deep Transfer Learning. *IEEE Transactions on Industrial Informatics*, 20 (1). pp. 399-410. ISSN 1551-3203

<https://doi.org/10.1109/TII.2023.3262856>

© 2023 IEEE. Personal use of this material is permitted. Permission from IEEE must be obtained for all other uses, in any current or future media, including reprinting/republishing this material for advertising or promotional purposes, creating new collective works, for resale or redistribution to servers or lists, or reuse of any copyrighted component of this work in other works.

Reuse

Items deposited in White Rose Research Online are protected by copyright, with all rights reserved unless indicated otherwise. They may be downloaded and/or printed for private study, or other acts as permitted by national copyright laws. The publisher or other rights holders may allow further reproduction and re-use of the full text version. This is indicated by the licence information on the White Rose Research Online record for the item.

Takedown

If you consider content in White Rose Research Online to be in breach of UK law, please notify us by emailing eprints@whiterose.ac.uk including the URL of the record and the reason for the withdrawal request.



eprints@whiterose.ac.uk
<https://eprints.whiterose.ac.uk/>

SFR Modelling for Hybrid Power Systems Based on Deep Transfer Learning

Jianhua Zhang, *Member, IEEE*, Yongyue Wang, Hongrui Li, Guiping Zhou, Bin Li, Lei Wang and Kang Li, *Senior Member, IEEE*

Abstract—A deep transfer learning method is presented for establishing the aggregated system frequency response (SFR) model of wind-thermal hybrid power systems (HPSs). In order to deal with nonlinearities and non-Gaussian disturbances, the quadratic survival information potential (QSIP) of the squared identification error is employed to construct the performance index when training recurrent neural networks (RNNs). A pre-trained SFR model is then obtained by the improved RNNs using the source domain data collected from the HPS in historical scenarios. Subsequently, the maximum mean difference is utilized to test the similarity of the HPS in historical and current scenarios. After that, the pre-trained SFR model is fine-tuned by adding some nodes to the recurrent layer and a functional link to the input layer. The SFR model of the HPS operating in current scenario can then be built based on the transferred source domain pre-trained SFR model. Simulation results illustrate that the proposed data driven modelling method can obtain accurate, effective and timely SFR model for a wind-thermal HPS with different wind speeds and load disturbances.

Index Terms—System frequency response; Power system modelling; System identification; Deep neural networks; Transfer learning

I. INTRODUCTION

IN order to incorporate more renewable energy based generation units in power grids, the concerns on frequency response are raised [1-2]. The imbalance between power generation and load will potentially cause frequency deviations. As a result, it is necessary to study the dynamic characteristics of system frequency under the disturbance of generation or load.

Investigation on power system frequency response (SFR) can reveal the dynamic characteristics of system frequency under the disturbance of generation or load, some approaches to SFR modelling have been presented [3-19].

This work was supported in part by National Key R&D Program of China No.2019YFB1505400. (Corresponding author: Jianhua Zhang)

J. H. Zhang is with the State Key Laboratory of Alternate Electrical Power System with Renewable Energy Sources, North China Electric Power University, Beijing, 102206, China (email: zjh@ncepu.edu.cn).

Y. Y. Wang is with the School of Control and Computer Engineering, North China Electric Power University, Beijing, 102206, China.

H. R. Li is with the State Power Investment Corporation Limited, Beijing, 100029, China.

G. P. Zhou, L. Wang and B. Li are with the State Grid Liaoning Electric Power Supply Co. Ltd., Shenyang, 110006, China.

K. Li is with School of Electronic and Electrical Engineering,

University of Leeds, LS2 9JT, UK.

The existed power system frequency response modelling approaches can be classified as three categories: direct measurement method [3-6], mechanism analysis method [7-15] and data-driven method [16-19].

1) Direct measurement method. This nonparametric method mainly investigates SFR by using Wide-Area Measurement System (WAMS) Data [3-5] and direct current load flow [6]. It is convenient and with low computational complexity, however, the relationship between frequency and generation/load can't be revealed explicitly, although the variations of frequency, generation and load along with time can be plotted clearly.

2) Mechanism analysis method. This method usually builds physical model to characterize dynamic SFR based on mechanism analysis. Some necessary assumptions and simplifications are required. The dynamic characteristics of each element of the HPS is taken into account, the overall physical model is then obtained by integrating all elements. Full model is usually established for developing power system simulation software, although this physical model has higher accuracy, however, it leads to larger computation burden. As a consequence, some equivalent models which take less computation cost have been built. Three kinds of average SFR model were presented in terms of delay model, canonical and hybrid delay-canonical model [7], in which all generators are aggregated into one equivalent rotor model, while the governor model of each generating unit is retained. Later, under the assumption that the generation is dominated by reheat steam turbine generators, a low order SFR model was proposed for large power systems in which most of the generating units are reheat steam turbine units [8]. Following the SFR models in [7] and [8], several extended SFR models were built for HPSs with renewable energy sources [9-14]. A modified average SFR model was presented for bulk power systems with doubly fed induction generator (DFIG)-based wind farms [9], this SFR model was used to evaluate short-term frequency regulation for the power system with wind farm. Authors in [10] and [11] integrated simplified models of wind turbines with other conventional sources. A low-order SFR model was built to represent AC frequency and DC voltage interaction for wind farms and voltage source converter-based high voltage direct current participating in primary frequency regulation [12]. The work in [13] established an extend SFR model for hybrid power systems (HPSs) with high penetration wind power considering

operating regions and wind speed disturbance. Reference [14] studied SFR of HPSs in the presence wind power and built a state-space model instead of transfer functions. Recently, an extended SFR model was proposed to evaluate SFR of cold load pickup following a large-scale blackout, in which a reduced first-order governor model was employed while the load model was built for considering time-dependent characteristic of inrush power surges [15]. These aforementioned low-dimension SFR models sacrifices model accuracy without considering nonlinearities and stochastic disturbances.

3) Data-driven method. This empirical approach usually utilizes input-output data to reveal the relationship between the inputs (generation and/or load) and the output (system frequency), which can significantly simplify the model structure with fewer computation resources. The data-driven model, also named as a black-box, needn't fully understand the detailed mechanisms of SFR. A generic SFR model was proposed for HPSs including thermal, hydro and renewable generation, in which the model parameters were identified using least square method [16]. The study in [17] developed a parabolic approximation of the SFR to obtain an explicit function of the frequency nadir using three points, subsequently, photovoltaic system power reserve was determined based on the approximated SFR. Authors in [18] utilized support vector regression (SVR) to predict power system frequency dynamics and its nadir after disturbances. In [19], an improved radial basis function neural networks was employed to model SFR of a wind-thermal hybrid power system (HPS). The data-driven model in [16-19] described frequency behavior in the vicinity of a certain scenario based on collected input-output data. The accuracy of the data-driven model is related to the number of samples available to train the model. However, in practical HPSs, the operating scenario always varies, the constructed off-line model doesn't necessarily describe SFR in another scenario properly due to lacking of extrapolating capability. Under this circumstance, the data-driven model should be established by training the collected input-output data corresponding to new scenario. To acquire enough data is time-consuming, difficult even in a short time. Unfortunately, the accuracy of the data-driven SFR model may not be guaranteed when the input-output data is inadequate.

High accuracy of SFR model and low computation effort are expected when modelling SFR of the wind-thermal HPSs. To address the gaps in the present literature, recurrent neural networks (RNNs) and transfer learning (TL) are employed to model SFR for HPSs.

Recurrent neural networks contain feedback connections among the neurons and can be used as identifiers and predictors in nonlinear dynamical systems [20-22]. In this context, RNNs is employed to build discrete state space SFR models for wind-thermal HPSs. Moreover, minimum mean squared error (MSE) adaptation is replaced by survival information potential (SIP) of the squared identification error to deal with non-Gaussian disturbances [23]. Although building RNNs based SFR model needs adequate and effective training data, however, to collect enough data from a new scenario is time-consuming and economically inefficient. As a result, it is necessary to

investigate data driven SFR modelling method when lack of adequate data.

Transfer learning can improve learning performance by avoiding much expensive data-collecting efforts and make some progress for solving classification, regression and clustering problems [24]. An attempt to build transfer learning based process model has been appeared in literature [25], in which source knowledge was incorporated based on Gaussian process model, and a dynamic transfer modelling approach was then proposed. In [26], transfer learning was used to improve a new building energy prediction accuracy by utilizing the collected data from other similar buildings when only limited data can be collected for the new building. It has been observed that deep transfer learning technology offers benefits in the area of fault diagnosis [27-28]. In [27], deep transfer learning based machine fault diagnosis method was presented, in which the pre-training network was employed to extract low-level features while the high-level network structure was fine tuned. In [28], a new method for fault diagnosis of machines with unlabelled data was proposed by using a deep convolutional transfer learning network.

Following the advancement in RNNs and deep transfer learning, we proposed a novel data driven modelling method to embrace the existing challenges when modelling SFR for HPSs. The main contributions include:

- 1) By incorporating transfer learning into RNNs with functional link, a data-driven modelling method is proposed to build SFR model for wind-thermal HPSs.
- 2) The pre-training RNNs can establish discrete state space SFR model for HPSs operating in specific scenarios by minimizing the quadratic survival information potential (QSIP) of the squared identification error.
- 3) Based on the maximum mean discrepancy (MMD) criterion, transfer learning is employed to improve the transferability of the fine-tuned RNNs based SFR model.
- 4) Compared with recent deep learning approaches, the proposed data driven SFR modelling method leads to more accurate results. Moreover, based on Sobol sensitivity analysis, the impact of the uncertainties of load and wind speed on modelling SFR is assessed, and the robustness of the proposed method to the impact of uncertainties is validated.

The rest of the paper is organized as follows. Section II reports the data-driven SFR intelligent modelling scheme of HPSs. Section III describes the deep transfer learning based SFR modelling method, followed by the simulation results and analysis in Section IV. Section V concludes this paper.

II. DATA-DRIVEN SFR INTELLIGENT MODELLING SCHEME

Deep transfer learning is a promising way to build SFR model for HPSs. The dynamic characteristics of wind-thermal HPSs are complicated in terms of time-varying, nonlinearities, uncertainties, intermittence and so on. Therefore, a deep transfer learning based intelligent modelling scheme is presented for HPSs in this section.

Figure 1 illustrates the schematic diagram of deep transfer learning based SFR modelling for a wind-thermal HPS. The overall load would be balanced by a wind-thermal hybrid power

plant at the point of common coupling. The hybrid power plant consists of a wind farm and a thermal power plant. There are multiple doubly fed induction generator (DFIG) based wind turbine generators and their primary frequency controls in the wind farm. The thermal power plant includes multiple synchronous generators and their steam governor controls.

The goal of this work is to build a deep transfer learning based system frequency response model that can accurately and quickly analyse the frequency dynamics of HPSs in the time scale of primary frequency regulation. To achieve the goal, the SFR model with three input variables (wind farm power change ΔP_W , mechanical power change of thermal power plant ΔP_M and load change ΔP_L) and one output variable (system frequency deviation Δf) will be obtained at offline and online stage respectively. Denote the identified system deviation as $y(k)$. For a start, an improved RNNs is employed to obtain the pre-trained SFR model at offline stage. Afterwards, nonlinear input transformation and transfer learning are incorporated into the pre-trained RNNs based SFR model, the fine-tuned strategy is presented for building SFR model at online stage. As a result, the dynamic frequency characteristics of an HPS can be analysed with the aid of the on line SFR model.

III. DEEP TRANSFER LEARNING BASED SFR MODELLING

In this section, deep transfer learning based SFR modelling method is elaborated, whose schematic diagram is depicted in Fig. 2. In Section III-A, the pre-trained offline SFR model is obtained by RNNs using source data. In Section III-B, the principle of transfer learning is presented, and then the deep transfer learning based online SFR model is obtained by fine-tuned RNNs using target and source data together.

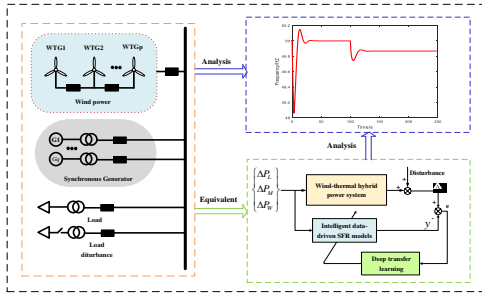


Fig. 1. Schematic diagram of building the SFR model.

The procedures including offline and online stages are described as follows:

Step 1: Historical input-output data is collected from the hybrid power system operating in some specific scenarios and pre-processed, denote it as source data.

Step 2: An improved RNNs are employed to build pre-trained SFR model by training source data.

Step 3: The online input-output data is collected from the hybrid power system operating in current scenario and pre-processed, denote it as target data.

Step 4: Analyze the data distribution discrepancy between source and target domain using MMD criterion.

Step 5: Make re-training strategy by fine tuning and

determine the frozen layer, the transferred knowledge or reinitialized information.

Step 6: Based on the pre-trained SFR model, the above re-training strategy in step 5 is used to obtain online SFR model using source data and target data together.

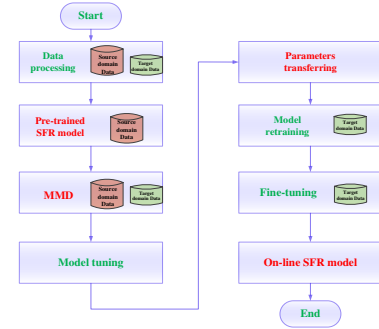


Fig. 2. Deep transfer learning based SFR modelling.

A. Pre-trained Offline SFR Model

The pre-trained SFR model is developed based on the collected data in the source domain. In this work, the collected data from the HPSs operating in some specific scenarios are pre-processed and saved in the source domain. The RNNs consists of one input layer, three hidden layers, and one output layer respectively, whose signal flow chart is shown in Fig. 3. The pre-trained offline SFR model is obtained by the RNNs shown in Fig. 4. RNNs can build mapping and capture time correlation in data sequence. A sequence of length $3T$ included by wind farm power change ΔP_W , mechanical power change of thermal power plant ΔP_M and load change ΔP_L is input to the RNNs, i.e. $u(k) = [\Delta P_M(k - T + 1), \Delta P_W(k - T + 1), \Delta P_L(k - T + 1), \Delta P_M(k), \Delta P_W(k), \Delta P_L(k)]^T \in R^{3T \times 1}$ is the input sequence at instant k . Three hidden layers shown in Fig. 3 is composed of one recurrent layer and two fully connected layers. The unique output in the output layer is the identified frequency deviation of the wind-thermal HPS at instant k . Consequently, the frequency deviation can be identified via the RNNs using the collected data from the wind-thermal HPS operating in some specific scenarios.

$$I(k) = g(W_{iu}u(k) + b_i) \quad (1)$$

$$X(k) = g(W_{xi}I(k) + W_{xx}X(k-1) + b_x) \quad (2)$$

$$C(k) = g(W_{cx}X(k) + b_c) \quad (3)$$

$$F(k) = g(W_{fc}C(k) + b_f) \quad (4)$$

$$y(k) = W_{yf}F(k) + b_y \quad (5)$$

where $I(k)$ is the output of the input layer. $X(k)$, $C(k)$ and $F(k)$ are the output of the hidden layers at instant k respectively. $W_{iu}, W_{xi}, W_{xx}, W_{cx}, W_{fc}$ and W_{yf} stand for the corresponding weights between adjacent layers. b_i, b_x, b_c, b_f and b_y are the corresponding biases. The activation function is a sigmoid function $g(z) = \frac{1}{1+e^{-z}}$. Hence, the following state space model (6) can be established from (1) and (2). In addition, the output (7) can be obtained by substituting (3) and (4) to (5).

$$X(k) = f(X(k-1), u(k)) \quad (6)$$

$$y(k) = h(X(k), u(k)) \quad (7)$$

Most of the existing works have assumed that the stochastic disturbances in HPSs are Gaussian, the mean value and variance of the signal are used to describe its randomness. However, the system frequencies of HPSs with renewable energy are non-Gaussian [31]. Hence, the mean value and variance of the system sequency cannot describe it completely and precisely.

Minimum error entropy (MEE) criterion has been employed to design controller or filter for non-Gaussian systems because entropy provides generalized randomness measure by its dispersion instead of mean or variance [32]. The global minimum corresponding to δ distribution under MEE criteria locates any position, so an additional bias term is needed due to the shift-invariant property. Accordingly, the survival information potential (SIP) of error has been presented to replace MEE [19, 23].

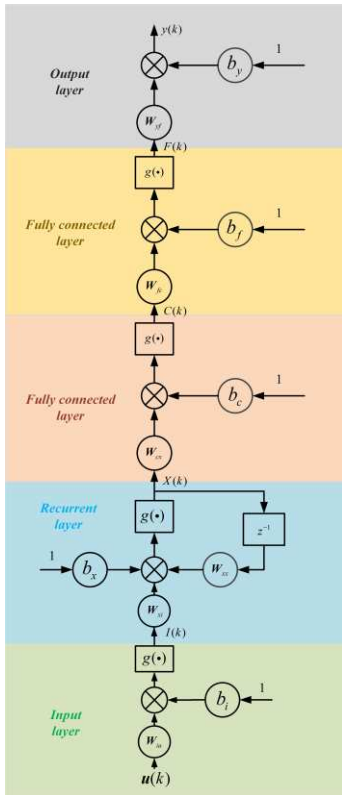


Fig. 3. The signal flow chart of RNN.

In this context, the quadratic survival information potential (QSIP) of the squared identification error is utilized to deal with non-Gaussian disturbances in HPSs. Denote the real frequency deviation as $\Delta f(k)$. Hence, the identification error is

$$e(k) = y(k) - \Delta f(k) \quad (8)$$

the QSIP of the squared identification error is regarded as the cost function to train the RNNs. It can be estimated using the sequential data collected by sliding window technique

$$J(k) = \sum_{j=k-T+1}^k \lambda_j e^2(j) \quad (9)$$

$$\text{where } \lambda_j = \left(\frac{k-j+1}{T} \right)^2 - \left(\frac{k-j}{T} \right)^2.$$

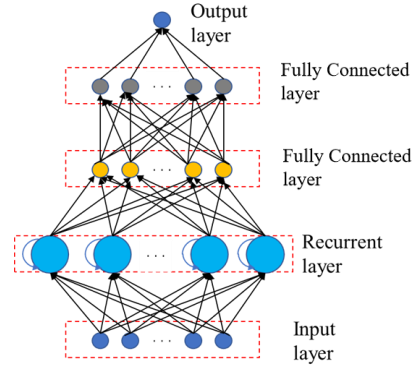


Fig. 4. RNNs for pre-trained SFR model framework.

The RNNs based SFR model is trained by backpropagation through time (BPTT) algorithm. Let the learning rate be η . The weights and biases of the RNNs can be obtained by minimizing the cost function (9).

The input-output data were collected from HPSs operating in historical scenarios and stored in source domain. These data in the source domain are represented by $\mathcal{D}_S = \{u_s, y_s\}$. The BPTT algorithm is used to build SFR models for wind-thermal HPSs.

B. Deep Transfer Learning Based Online SFR Model

Most of data-driven methods re-train model using online data. However, unnecessary data updating and re-training is usually costly and time-consuming. Transfer learning can be used to address this problem. In addition, when the input-output data of the investigated wind-thermal HPS operating in current scenario is limited, the sufficient data collected in historical scenarios are helpful to build the online SFR model for the HPS operating in current scenario. Transfer learning can transfer knowledge from historical data to improve online SFR modelling abilities.

Denote the input-output data in current scenario as the target domain $\mathcal{D}_T = \{u_t, y_t\}$. Transfer learning is incorporated into the pre-trained RNNs to establish the online SFR model by using target data and source data together.

In order to deal with a domain shift between source domain \mathcal{D}_S and target domain \mathcal{D}_T , maximum mean discrepancy (MMD) based domain adaptation algorithm is presented for online SFR modelling. MMD defined in [29] is a distribution distance metric to compare the distributions between two datasets using a kernel two-sample test.

$$\begin{aligned} MMD^2[\mathcal{D}_S, \mathcal{D}_T] &= \left\| \frac{1}{n_s} \sum_{i=1}^{n_s} \phi(x_s^i) - \frac{1}{n_t} \sum_{i=1}^{n_t} \phi(x_t^i) \right\|_H^2 \\ &= \left[\frac{1}{m(m-1)} \sum_{i \neq j}^m k(x_s^i, x_s^j) + \frac{1}{n(n-1)} \sum_{i \neq j}^n k(x_t^i, x_t^j) \right. \\ &\quad \left. - \frac{2}{mn} \sum_{i,j=1}^{m,n} k(x_s^i, x_t^j) \right] \end{aligned} \quad (10)$$

where ϕ is the kernel function that maps the original data to a

reproducing kernel Hilbert space, $k(x, x') = \exp\left(-\frac{\|x - x'\|^2}{2\sigma^2}\right)$.

Since MMD criterion can be used to measure the discrepancy between source domain \mathcal{D}_S and target domain \mathcal{D}_T , it can be regarded as the transfer criterion from \mathcal{D}_S to \mathcal{D}_T . The pre-trained RNNs can be fine-tuned while the parameters obtained in the pre-trained RNNs are migrated selectively. The domain adaption MMD is classified into three cases:

Case 1: The data distributions of source domain \mathcal{D}_S and target domain \mathcal{D}_{T_1} are similar if MMD is less than the pre-specified threshold α , the parameters of the pre-trained RNNs can then be fine-tuned. The deep transfer learning based online SFR modelling process includes two stages: the pretraining on source domain \mathcal{D}_S and the fine-tuning on target domain \mathcal{D}_{T_1} . The pretrained RNNs based SFR model is frozen when finishing pretraining RNNs. The fine-tuning method in this case focuses on determining the additional recurrent nodes via transfer learning method. Subsequently, the additional recurrent nodes are integrated to the frozen pretrained RNNs. Denote the fine-tuned RNNs based SFR model as Model A. As a sequence, the online SFR model can be obtained via Model A.

Case 2: The data distributions of source domain \mathcal{D}_S and target domain \mathcal{D}_{T_2} are dissimilar if MMD is greater than the pre-specified threshold α and less than the pre-specified threshold β , the SFR modelling method is shown in Fig. 5. The transfer learning based online SFR modelling process includes two stages: the pretraining on source domain \mathcal{D}_S and the fine-tuning on target domain \mathcal{D}_{T_2} . The fine-tuning method in this case not only adds appropriate recurrent nodes but also performs nonlinear input transformation. Denote the fine-tuned SFR model shown in Fig. 5 as Model B. Nonlinear input transformation is performed on each input node by a trigonometric polynomial basis function $\{1, \sin(\pi u(k)), \cos(\pi u(k)), \sin(2\pi u(k)), \cos(2\pi u(k)), \dots, \sin(N_L \pi u(k)), \cos(N_L \pi u(k))\}$, which provides a compact representation of the function in the mean square sense [30]. The input transformation with functional link has fast convergence rate and less computational burden [30]. Compromising between complexity and accuracy, the order of the nonlinear expansion using trigonometric functions N_L , is selected by trail and error method. In addition, the additional recurrent nodes RNNs shown in green is also fine-tuned using trail and error method.

Case 3: If MMD is much greater than the pre-specified threshold β , the transfer learning based SFR model shown in Fig. 4 cannot obtain satisfactory model accuracy. Accordingly, the pre-trained SFR model should be modified using proper source data.

IV. RESULTS AND DISCUSSIONS

The following tests were conducted to testify the effectiveness of the proposed deep transfer learning based SFR modelling algorithm. In addition, to provide a sufficient comparison, RNNs under MSE criterion, RNNs under SIP criterion are also implemented. The experimental wind-thermal HPS is shown in Fig. 1 ($p=200, q=2$). There are $200 \times 1.5\text{MW}$

DFIG wind turbine generators in the wind farm. Each wind turbine generator adopts same primary frequency regulation. The constant gain of the droop control is set to $K_w = 50 \text{ MW/Hz}$. The detailed general non-linear wind turbine generator model of a DFIG wind turbine generator is given in [33], the corresponding parameters are listed in Table I. There are two 600MW reheat steam generator units in the thermal power plant. Each reheat steam generator unit is equipped with a prime mover speed control system and excitation voltage regulator. The adjustment coefficients of the steam turbine governing system are set to $K_t = 20 \text{ MW/Hz}$. The model parameters of the reheat steam generator unit are given in Table II.

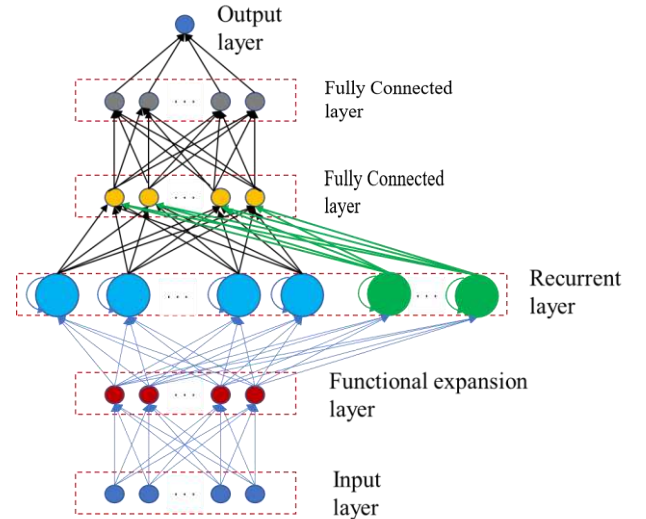


Fig. 5. Transfer learning based Online SFR model.

TABLE I
PARAMETERS OF DFIG WIND TURBINE GENERATOR

Variable	Parameters values	Variable name	Parameters values
Rated voltage	690V	Rotor resistant	0.016p.u
Rated power	1.5MW	Rotor leakage inductance	0.156p.u
Stator resistant	0.00706p.u	Rated wind speed	12m/s
Stator leakage inductance	0.171p.u	Performance coefficient of the turbine	0.73p.u

In this simulation, the sampling period is set to 0.1s. The width of the sliding window is set to 100, the data within the sliding window is used to estimate the SIP of the squared identification error. The length of the sequential data in the input layer is set to $T = 10$. The weights of the RNNs are initialized as random numbers within a range $[-1, 1]$. Two pre-specified thresholds are set to $\alpha = 0.1$ and $\beta = 0.3$ by trial and error respectively.

TABLE II
PARAMETERS OF THERMAL POWER UNIT

Variable	Value	Variable	Value
Governor time constant	0.18s	High-pressure turbine fraction	0.33

Steam chest time constant	0.2s	Governor speed regulation	0.05
Reheat time constant	11.27s	Load damping factor	0.02

A. Typical Scenarios and Dataset Description

The typical scenarios of the wind-thermal HPS are characterized by wind speed and load disturbance. Three kinds of typical scenarios are investigated as shown in Table III. Random variables $\beta_1, \beta_2, \beta_3$ and β_4 uniformly distribute on the intervals $[-0.5, 0.5]$, $[-100, 100]$, $[-110, 110]$, and $[-120, 120]$, respectively. In this work, k -fold cross-validation is utilized. The dataset \mathcal{D}_S , \mathcal{D}_{T1} and \mathcal{D}_{T2} are split into 10 batches of similar sizes respectively. When looping over $l = 1, 2, \dots, 10$, batch l is held out as validation data, and the model is trained on the remaining 9 data batches and the trained model is used to compute the performance evaluation metrics for the validation data. The final SFR model is trained using all available data, and the performance evaluation metrics for the final SFR model are the average of all loops. For brevity, not all the test results are summarized here, only the typical results in current case for each scenario are reported.

B. Model Accuracy Evaluation

In order to evaluate the accuracy of the established model, root mean square error (RMSE), mean absolute error (MAE), determination coefficient R^2 and mean absolute percent error (MAPE) are used as performance evaluation metrics.

(1) RMSE is the expected value of the square of the difference between the identified frequency deviation and actual frequency deviation.

$$RMSE = \sqrt{\frac{1}{n} \sum_{i=1}^n (y_i - \Delta f_i)^2} \quad (11)$$

(2) MAE can better reflect the actual situation of the predicted error

$$MAE = \frac{1}{n} \sum_{i=1}^n |y_i - \Delta f_i| \quad (12)$$

(3) The determination coefficient represents the quality of a fitting through the change of data.

$$R^2 = 1 - \frac{\sum_{i=1}^n (y_i - \Delta f_i)^2}{\sum_{i=1}^n (y_i - \bar{y})^2} \quad (13)$$

(4) MAPE is the summary measure for evaluating model accuracy

$$MAPE = \frac{1}{n} \sum_{i=1}^n \left| \frac{y_i - \Delta f_i^c}{\Delta f_i} \right| \quad (14)$$

TABLE III
THREE TYPICAL SCENARIOS IN THE TEST

Scenario	Group of time series data	Wind speed m/s	Load disturbance MW
1	3500 in \mathcal{D}_S	$10 + \beta_1$	$1000 + \beta_2$
2	500 in \mathcal{D}_{T1}	$10.5 + \beta_1$	$1000 + \beta_3$
	Current case	10.5	1000 ± 110

3	500 in \mathcal{D}_{T2}	$12 + \beta_1$	$1000 + \beta_4$
	Current case	12	1000 ± 120

Scenario 1: The wind-thermal HPS operated in the vicinity of the operating point featured by wind speed 10 m/s and load 1000 MW. The uniformly distributed random disturbances were imposed on wind speed and load, respectively, whose perturbation ranges are $[-0.5\text{m/s}, 0.5\text{m/s}]$ and $[-100\text{MW}, 100\text{MW}]$ respectively. 3500 groups of input-output data were collected and denoted as source data \mathcal{D}_S . The appropriate learning rate and recurrent node number can be determined during training stage using trail and error method. 3150 groups training data selected from the dataset \mathcal{D}_S were input to the RNNs, the average RMSE of the RNN with different recurrent node number is shown in Table IV when the learning rate $\eta = 0.05$ remains unchanged. It can be observed that 8 recurrent nodes can achieve the lowest RMSE. Table V shows the average RMSE with different learning rates when the number of recurrent nodes is fixed to 8, it is clear that the learning rate can be set to $\eta = 0.07$. Finally, the pre-trained RNNs can model SFR of the wind-thermal HPS.

TABLE IV
AVERAGE RMSE WITH DIFFERENT NEURONS IN RECURRENT LAYER

Number of neurons in recurrent layer	5	6	7	8	9
RMSE	1.93e-4	1.55e-4	1.28e-4	9.62e-5	1.46e-4
Number of neurons in recurrent layer	10	11	12	13	14
RMSE	1.63e-4	2.07e-4	2.23e-4	2.28e-4	2.96e-4

Note: The bold entities denote the lowest error among the various number of neurons in recurrent layer.

TABLE V
AVERAGE RMSE WITH DIFFERENT LEARNING RATES

The learning factor	0.01	0.02	0.03	0.04	0.05
RMSE	3.89e-4	3.33e-5	2.65e-4	2.37e-4	1.63e-4
The learning factor	0.06	0.07	0.08	0.09	0.1
RMSE	8.68e-5	7.25e-5	9.61e-5	2.21e-4	4.23e-4

Note: The bold entities denote the lowest error among the various learning rates.

In addition, deep belief network (DBN) [34], deep temporal dictionary learning (DTDLD) [35], sparse autoencoder (SAE) [36] and rough autoencoder (RAE) [37] are introduced for comparison. The performance evaluation metrics are listed in Table VI. It can be observed from Table VI that the proposed method can obtain the most accurate SFR model.

TABLE VI
PERFORMANCE EVALUATION METRICS OF FINAL MODEL

Method	Accuracy			
	RMSE	MAE	R^2	MAPE
RNN-MSE	1.13e-4	8.28e-5	0.970	0.237
RNN-SIP	8.79e-5	5.83e-5	0.982	0.149

DBN	4.171e-4	3.139e-4	0.515	0.982
SAE	1.99e-4	1.41e-4	0.868	0.512
DTDl	6.19e-4	6.01e-4	0.408	0.991
RAE	2.14e-4	1.71e-4	0.849	0.835

Scenario 2: The HPS operated in the vicinity of the operating point featured by wind speed 10.5 m/s and load 1000 MW. 500 groups of input-output data with uniformly distributed random disturbances shown in Table III were collected and denoted as target data \mathcal{D}_{T1} . It follows from Eq. (10) that the discrepancy between source domain and target domain can be obtained $MMD=0.065$.

Frozen the pretrained RNNs obtained in scenario 1, the fine-tuned SFR model A can be established by adding appropriate recurrent nodes to the frozen RNNs. 450 groups training data selected from the dataset \mathcal{D}_{T1} were input to the RNNs. Two additive recurrent nodes were selected by trial and error method. The transfer learning based SFR model A was obtained in the end.

By performing nonlinear input transformation and adding appropriate recurrent nodes to the frozen pretrained RNNs obtained in scenario 1, the fine-tuned SFR model B will be established. Two additive recurrent nodes were still selected using trial and error method. Three order trigonometric polynomial basis function applied to the input transformation is selected by trail and error method. In the end, the transfer learning based SFR model B was obtained. Table VII lists the performance evaluation metrics of model A and model B trained by the target data respectively. In current case, the wind speed was $v = 10.5\text{m/s}$ while the load disturbance ΔP_L shown in Fig. 6 fluctuated randomly between $[-0.11, 0.11]$ p.u. Figure 7 illustrates the real frequency deviation and the identified frequency deviations obtained by model A and model B. It can be seen from Fig. 7 that model A can approximate real frequency better than model B. The PDFs of the identification error γ_e at typical instants is shown in Fig. 8. The PDFs of the identification error obtained by Model A are narrower and sharper. In addition, Table VIII lists the performance evaluation metrics of Model A and Model B respectively. Obviously, model A outperforms Model B.

Scenario 3: The HPS operated in vicinity of the operating point with the wind speed $v = 12\text{m/s}$ and load 1000 MW. 500 groups of input-output data uniformly distributed random disturbances shown in Table III were collected and denoted as target data \mathcal{D}_{T2} . $MMD=0.224$ can be obtained by Eq. (10).

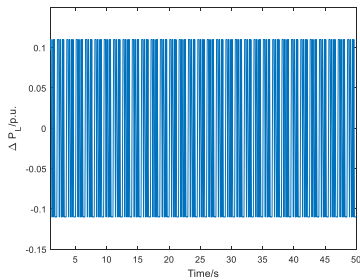


Fig. 6. Load disturbances in scenario 2.

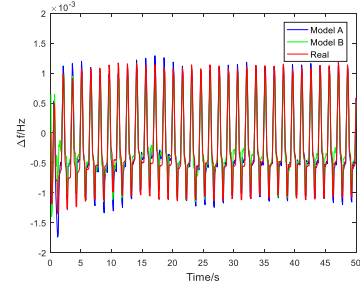
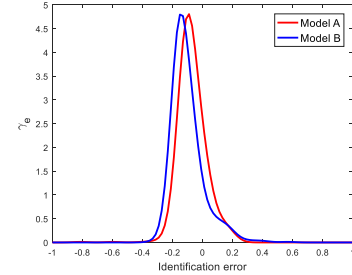
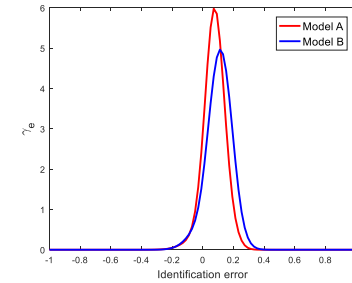
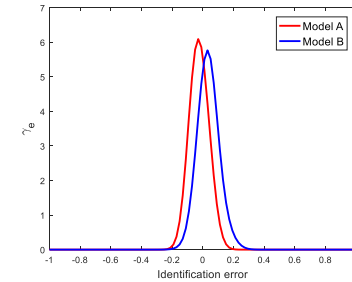


Fig. 7. Curves of frequency deviation.

(a). γ_e at $t=10\text{s}$.(b). γ_e at $t=20\text{s}$.(c). γ_e at $t=50\text{s}$.Fig. 8. γ_e at typical instants.TABLE VII
PERFORMANCE EVALUATION METRICS OF FINAL MODEL

Model	Accuracy			
	RMSE	MAE	R^2	MAPE
Model A	9.86e-5	8.32e-5	0.970	0.236
Model B	1.37e-4	9.55e-5	0.958	0.352

TABLE VIII
PERFORMANCE EVALUATION METRICS IN CURRENT CASE

Model	Accuracy			
	RMSE	MAE	R^2	MAPE
Model A	8.98e-5	6.02e-5	0.981	0.159

Model B	1.0e-4	7.55e-5	0.971	0.210
---------	--------	---------	-------	-------

Frozen the pretrained RNNs obtained in scenario 1, the fine-tuned SFR model A can be built by adding appropriate recurrent nodes to the frozen RNNs. 450 groups training data selected from the dataset \mathcal{D}_{T2} were input to the RNNs. Three additive recurrent nodes were selected using trial and error method, and then the transfer learning based SFR model A was obtained.

By conducting nonlinear input transformation and fine-tuning appropriate recurrent nodes to the frozen pretrained RNNs obtained in scenario 1, the fine-tuned SFR model B will be established using the dataset \mathcal{D}_{T2} . Three additive recurrent nodes and three order of the nonlinear input transformation were selected by trial and error method. Table IX lists the average performance evaluation metrics of the transfer learning based SFR model A and model B. In current case, the wind speed was $v = 12\text{m/s}$ while the load disturbance ΔP_L shown in Fig. 9 varied in the vicinity of $[-0.12, 0.12]$ p.u. Figure 10 demonstrates the identified frequency deviations by model A and model B besides the real frequency deviation. It can be observed from Fig. 10 that Model B can approximate real frequency better than model A. The PDFs of the identification error γ_e at typical instants is shown in Fig. 11. The PDFs of the identification error obtained by Model B are narrower and sharper. Table X lists the comparison between Model A and Model B. It is clear that model B is better than Model A in this scenario.

In summary, these simulation results illustrate the relationship between the selected model and MMD. When the MMD of source domain \mathcal{D}_S and target domain \mathcal{D}_T is less than the pre-specified threshold α , the SFR model can obtain better performance using model A. It means that scenario 2 is close to

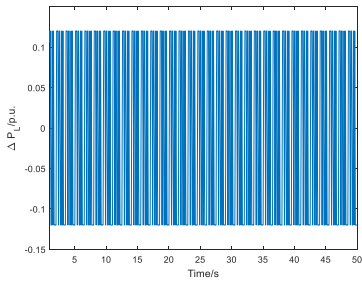


Fig. 9. Load disturbances scenario 3.

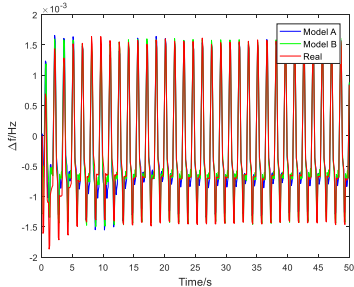
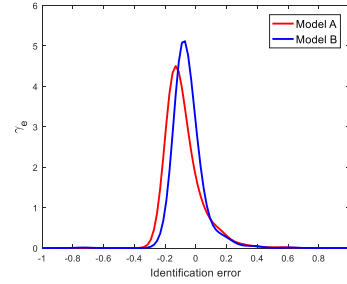
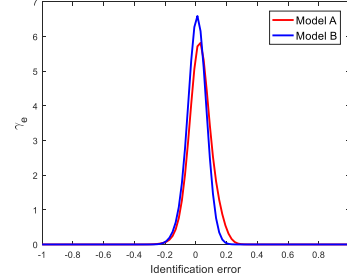


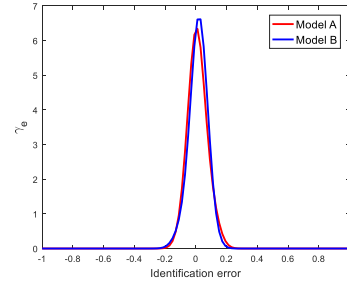
Fig. 10. Identification curve of frequency deviation.



(a). γ_e at $t=10\text{s}$.



(b). γ_e at $t=20\text{s}$.



(c). γ_e at $t=50\text{s}$

Fig. 11. γ_e at typical instants.

historical scenario in source domain, it is not necessary to add functional link. On the other hand, when the MMD in scenario 3 is greater than the pre-specified threshold α and less than the pre-specified threshold β , model fine-tuning shown in Fig. 4 should be performed because of the dissimilarity between current scenario and historical scenario. It is clear that model B can reflect SFR of the wind-thermal HPS better than Model A.

TABLE IX
PERFORMANCE EVALUATION METRICS OF FINAL MODEL

Model	Accuracy			
	RMSE	MAE	R^2	MAPE
Model A	1.83e-4	1.36e-4	0.951	0.196
Model B	1.66e-4	1.02e-4	0.964	0.188

TABLE X
PERFORMANCE EVALUATION METRICS IN CURRENT CASE

Model	Accuracy			
	RMSE	MAE	R^2	MAPE
Model A	1.59e-4	1.02e-4	0.968	0.183
Model B	1.46e-4	8.35e-5	0.973	0.179

C. Sensitivity Analysis

In order to show the robustness of the proposed method to uncertainties from load and wind speed in HPSs, the sensitivity analysis (SA) is conducted. This study performs the SA using the variance-based Sobol indices [38] owing to its straightforward interpretation. And these indices represent the contribution of a parameter noised by uncertainties to the overall decrease of the SFR modelling accuracy. The Sobol indices S_i measuring the sensitivity of the frequency deviation with respect to each input uncertain parameter X_i are given as (15).

$$S_i = \frac{\sigma^2_{X_i} \left(\mathbb{E}_{X_{-i}}(y | X_i) \right)}{\sigma^2(y)} \quad (15)$$

where the frequency deviation y is a random variable ; $\sigma^2(y)$ is the unconditional variance, $\mathbb{E}_{X_{-i}}(y | X_i)$ is the expected value of y conditional on X_i (i.e., X_i remains fixed), and $\sigma^2_{X_i} \left(\mathbb{E}_{X_{-i}}(y | X_i) \right)$ is the conditional variance of y caused by a variation of X_i .

In this work, two 500-samples of noisy validation datasets were collected to test the influence of uncertainties on the pre-trained model, Model A and Model B established respectively. Denote two independent sampling matrices \bar{A} and \bar{B} , with a_{ji} and b_{ji} as generic elements. The index i runs from 1 to 2, where X_1 and X_2 are non-Gaussian disturbances from load and wind speed, respectively. The index j runs from 1 to 500. We introduce matrix $\bar{B}_A^{(i)}$ where all columns are from \bar{B} except the i -th column which is from \bar{A} . $\sigma^2_{X_i} \left(\mathbb{E}_{X_{-i}}(y | X_i) \right)$ can then be computed as follows:

$$\sigma^2_{X_i} \left(\mathbb{E}_{X_{-i}}(y | X_i) \right) = \frac{1}{N} \sum_{j=1}^N f(\bar{A})_j f(\bar{B}_A^{(i)})_j - \mathbb{E}^2(y) \quad (16)$$

where ‘ f ’ is the model that links the inputs to the output, $\mathbb{E}(y)$ is the expected value of y .

The S_i takes a value between 0 and 1 because it is normalized by $\sigma^2(y)$. $S_i = 0$ indicates that the input uncertain parameters have no influence on the variance of output and $S_i = 1$ indicates that this input uncertain parameter is the full cause of the output variance.

Table XI shows the Sobol indices for three SFR models. As observed in Table XI, non-Gaussian load and wind speed disturbances both have small Sobol indices. Therefore, the influence of uncertainties on the precision of SFR model can be ignored, the established SFR models are robust to uncertainties from load and wind speed in wind-thermal HPSs.

TABLE XI
SOBOL INDICES FOR THE THREE SFR MODEL

Model	S1	S2
Pre-trained model	0.064	0.060
Model A	0.092	0.074
Model B	0.086	0.071

V. CONCLUSIONS

In this paper, a deep transfer learning based SFR modelling method is proposed for wind-thermal HPSs. It transfers source domain knowledge to the target domain, hence, the cost and the effort required to collect the SFR data are reduced. Simulation tests in a wind thermal HPS with different wind speeds and load disturbances have been conducted. The effectiveness of the established deep transfer learning based SFR model is also testified. The features of the proposed methods include:

1) The pre-trained SFR modelling method is given based on an improved RNNs. The QSIP of the squared identification error is introduced to construct the cost function for training RNNs, non-Gaussian disturbances in wind-thermal HPSs can then be coped with. Thus, the discrete state space SFR model can be build using the data from the HPS operating in historical scenarios.

2) The principle to transfer the knowledge of source domain is presented based on MMD. The transfer learning deals with transferring knowledge from historical scenarios to current scenario. The SFR of the HPS operating in current scenario can be represented by the fine-tuned RNNs, in which the nodes in recurrent layer are increased while the input nodes are expanded via functional link.

3) The proposed data driven SFR modelling method can build more accurate model, moreover, the SFR model is robust to the impact of uncertainties from load and wind speed in wind-thermal HPSs.

REFERENCES

- [1] X. Xu, W. Ming, Y. Zhou and J. Wu, "Unlock the flexibility of combined heat and power for frequency response by coordinative control with batteries," *IEEE Trans. Ind. Informat.*, vol. 17, no. 5, pp. 3209-3219, May 2021.
- [2] D. Andrew, *Modern aspects of power system frequency stability and control*, Western Pennsylvania Scholastic, WPS, USA: Academic Press; 2019.
- [3] K. Liu, X. Wang, "A wide-area measurement data based method for power system dynamic frequency analysis," *Power System Technology*, vol. 37, no. 8, pp. 2201-2206, Aug. 2013.
- [4] K. Liu, X. Wang and Q. Bo, "Minimum frequency prediction of power system after disturbance based on the WAMS data," *Proceedings of the CSEE*, vol. 34, no. 13, pp. 2188-2195, May.2014.
- [5] U. Rudez and R. Mihalic, "WAMS-based underfrequency load shedding with short-term frequency prediction," *IEEE Trans. Power Deliv.*, vol. 31, no. 4, pp. 1912-1920, Aug. 2016.
- [6] C. Li, Y. Liu and H. Zhang, "Power system frequency response analysis based on the direct current load flow," *Proceedings of the CSEE*, vol. 29, no. 34, pp. 36-41, Dec. 2009.
- [7] M. L. Chan, R. D. Dunlop and F. Schweppe, "Dynamic equivalents for average system frequency behavior following major disturbances," *IEEE Trans Power Syst*, vol. PAS-91, no. 4, pp. 1637-1642, Jul. 1972.
- [8] P. M. Anderson and M. Mirheydar, "A low-order system frequency response model," *IEEE Trans Power Syst*, vol. 5, no. 3, pp. 720-729, Aug. 1990.
- [9] M. Akbari and S. M. Madani, "Analytical evaluation of control strategies for participation of doubly fed induction generator based wind farms in power system short-term frequency regulation," *IET Renew Power Gener.*, vol. 8, no. 3, pp.324-333, Apr. 2014.

- [10] D. Ochoa and S. Martinez, "Fast-frequency response provided by DFIG-wind turbines and its impact on the grid," *IEEE Trans Power Syst*, vol. 32, no. 5, pp. 4002-4011, Sept. 2017.
- [11] C. Pradhan and C. N. Bhende, "Frequency sensitivity analysis of load damping coefficient in wind farm-integrated power system," *IEEE Trans Power Syst*, vol. 32, no. 2, pp. 1016-1029, March 2017.
- [12] H. Ye, W. Pei, L. Kong and T. An, "Low-order response modeling for wind farm-MTDC participating in primary frequency controls," *IEEE Trans Power Syst*, vol. 34, no. 2, pp. 942-952, March 2019.
- [13] J. Dai, Y. Tang, Q. Wang, P. Jiang and Y. Hou, "An extended SFR model with high penetration wind power considering operating regions and wind speed disturbance," *IEEE Access*, vol. 7, pp. 103416-103426, 2019.
- [14] N. Nguyen and J. Mitra, "An analysis of the effects and dependency of wind power penetration on system frequency regulation," *IEEE Trans Sustain Energy*, vol. 7, no. 1, pp. 354-363, Jan. 2016.
- [15] D. Rodriguez Medina et al., "Fast assessment of frequency response of cold load pickup in power system restoration," *IEEE Trans Power Syst*, vol. 31, no. 4, pp. 3249-3256, Jul. 2016.
- [16] H. Huang, P. Ju, Y. Jin, X. Yuan, C. Qin, X. Pan, and X. Zang, "Generic system frequency response model for power grids with different generations," *IEEE Access*, vol. 8, pp. 14314-14321, 2020.
- [17] T. Baškarad, I. Kuzle and N. Holjevac, "Photovoltaic system power reserve determination using parabolic approximation of frequency response," *IEEE Trans. Smart Grid*, vol. 12, no. 4, pp. 3175-3184, July 2021.
- [18] Q. Bo, X. Wang and K. Liu, "Minimum frequency prediction of power system after disturbance based on the v-support vector regression," 2014 International Conference on Power System Technology, 2014.
- [19] J. Zhang. "Modelling of SFR for wind-thermal power systems via improved RBF neural networks," Proceedings of 2020 Chinese Intelligent Systems Conference. CISC 2020. Lecture Notes in Electrical Engineering, vol 706. Springer, Singapore 2021.
- [20] D. P. Mandic, J. A. Chambers, Recurrent neural networks for prediction, John Wiley & Sons Ltd, 2001.
- [21] A. N. Michel, D. Liu, Qualitative Analysis and synthesis of recurrent neural networks, CRC Press, 2002.
- [22] F. M. Bianchi, E. Maiorino, M. C. Kampffmeyer, A. Rizzi, R. Jenssen, Recurrent neural networks for short-term load forecasting, Springer-Verlag London Limited, 2017.
- [23] B. Chen, P. Zhu and J. C. Principe, "Survival information potential: a new criterion for adaptive system training," *IEEE Trans Signal Process*, vol. 60, no. 3, pp. 1184-1194, March 2012.
- [24] S. J. Pan and Q. Yang, "A survey on transfer learning," *IEEE T Knowl Data En*, vol. 22, no. 10, pp. 1345-1359, Oct. 2010.
- [25] K. L. Wang, J. H. Chen, L. Xie, H. Su, " Transfer learning based on incorporating source knowledge using Gaussian process models for quick modeling of dynamic target processes, " *Chemometr Intell Lab Syst*, Vol. 198, 103911, 2020.
- [26] M. Ribeiro, K. Grolinger, H. F. Elyamany, W. A. Higashino, M. A. M. Capretz, "Transfer learning with seasonal and trend adjustment for cross-building energy forecasting, " *Energy Build*, Vol. 165, pp. 352-363, 2018.
- [27] S. Shao, S. McAleer, R. Yan and P. Baldi, "Highly accurate machine fault diagnosis using deep transfer learning," *IEEE Trans Industr Inform*, vol. 15, no. 4, pp. 2446-2455, April 2019.
- [28] L. Guo, Y. Lei, S. Xing, T. Yan and N. Li, "Deep convolutional transfer learning network: a new method for intelligent fault diagnosis of machines with unlabeled data," *IEEE Trans Indust Electron*, vol. 66, no. 9, pp. 7316-7325, Sept. 2019.
- [29] A. Gretton, K. M. Borgwardt, M. J. Rasch, B. Scholkopf, and A. J. Smola, "A kernel two-sample test," *Journal of Machine Learning Research*, vol. 13, pp. 723-773, 2012.
- [30] J. C. Patra, R. N. Pal, B. N. Chatterji and G. Panda, "Identification of nonlinear dynamic systems using functional link artificial neural networks," *IEEE Trans Syst Man Cybern*, vol. 29, no. 2, pp. 254-262, April 1999.
- [31] B. Schäfer, C. Beck, K. Aihara. "Non-Gaussian power grid frequency fluctuations characterized by Lévy-stable laws and superstatistics," *Nat Energy*, vol. 3, pp. 119-126, Jan 2018.
- [32] L. Guo, Y. Yi, and L. P. Yin, Modelling, analysis and control theories of Non-Gaussian distribution systems. Beijing, China: Science Press; 2019.
- [33] S. Li, Y. Huang. X. Lei and C. Deng, "Modeling primary frequency regulation auxiliary control system of doubly fed induction generator based on rotor speed control." *Proceedings of the Csee*, vol. 37, no. 24, pp. 7077-7086, Feb. 2017.
- [34] T. Ouyang, Y. He, H. Li, Z. Sun, and S. Baek, "Modeling and forecasting short-term power load with copula model and deep belief network," *IEEE Trans. Emerg*, vol. 3, no. 2, pp. 127-136, 2019.
- [35] M. Khodayar, J. Wang, and Z. Wang, "Energy disaggregation via deep temporal dictionary learning," *IEEE Trans Neural Netw Learn Syst*, vol. 31, no. 5, pp. 1696-1709, May 2020.
- [36] C. Sun, M. Ma, Z. Zhao, S. Tian, R. Yan, and X. Chen, "Deep transfer learning based on sparse autoencoder for remaining useful life prediction of tool in manufacturing," *IEEE Trans. Ind. Informat*, vol. 15, no. 4, pp. 2416-2425, 2019.
- [37] M. Khodayar, O. Kaynak, and M. E. Khodayar, "Rough deep neural architecture for short-term wind speed forecasting," *IEEE Trans. Ind. Informat*, vol. 13, no. 6, pp. 2770-2779, 2017.
- [38] W. Zouhri, L. Homri, and J.-Y. Dantan, "Handling the impact of feature uncertainties on SVM: A robust approach based on Sobol sensitivity analysis", *Expert Syst. Appl*, vol. 189, p. 115691, Mar. 2022.



Jianhua Zhang received the B.Sc. degree in Industrial Automation from North China Electrical Power College, Hebei, China, in 1990, the M.Sc. degree in Control Engineering from Beijing graduate school of North China Electrical Power College, Beijing, China, in 1993, and the Ph.D. degree in mechanical engineering from Beijing University of Aeronautics and Astronautics, Beijing, China, in 1996.

She is currently a Professor in the School of Control and Computer Engineering, North China Electric Power University, Beijing. Her research interests include the areas of integrated energy systems, stochastic control, networked control systems, power system and process control.



Yongyue Wang received the B.Sc. degree in Control Theory and Control Engineering from North China Electric Power University, Beijing, China, in 2020.

He is currently pursuing the Ph.D. degree in Control Theory and Control Engineering from North China Electric Power University. His research interests include hybrid power system, frequency regulation, neural networks, robust control, stochastic control and intelligent optimization.



Hongrui Li received the B.Sc. degree in Electrical Engineering and its Automation from LiRen College, Yanshan University, Qinhuangdao, China, in 2018, the M.Sc. degree in Control Theory and Control Engineering from North China Electric Power University, Beijing, China, in 2021.

He is currently working at State Power Investment Corporation Limited. His research interests include hybrid power system, frequency regulation and neural networks.



Guiping Zhou received the B.Sc. degree in Dalian University of Technology, Dalian, China, in 2004, the M.Sc. degree in Shenyang University of Chemical Technology, Shenyang, China, in 2007, and the Ph.D. degree in Shenyang Institute of Automation Chinese Academy of Sciences, Shenyang, China, in 1995.

He is currently working at the State Grid Liaoning Electric Power Supply Co. Ltd. His research interests include power system and automation.



Bin Li received the B.Sc. degree and the M.Sc. degree in College of Information Science and Engineering from Northeastern University, Shenyang, China, in 2004, and 2008, respectively, and the Ph.D. degree in School of Electrical Engineering from Shenyang University of Technology, Shenyang, China, in 2013.

He is currently working at the State Grid Liaoning Electric Power Supply Co. Ltd. His research interests include grid equipment status detection and fault

diagnosis.



Lei Wang received the B.Sc. degree in Harbin Engineering University, Harbin, China, in 2004, the M.Sc. degree and the Ph.D. degree in Harbin Institute of Technology, Harbin, China, in 2007, and 2011, respectively.

He is currently working at the State Grid Liaoning Electric Power Supply Co. Ltd. His research interests include network security management, network security architecture protection design, network and information

security technology.



Kang Li (M'05–SM'11) received the B.Sc. degree in Industrial Automation from Xiangtan University, Hunan, China, in 1989, the M.Sc. degree in Control Theory and Applications from Harbin Institute of Technology, Harbin, China, in 1992, and the Ph.D. degree in Control Theory and Applications from Shanghai Jiaotong University, Shanghai, China, in 1995. He also received D.Sc. degree in Engineering from Queen's University Belfast, UK, in 2015.

Between 1995 and 2002, he worked at Shanghai Jiaotong University, Delft University of Technology and Queen's University Belfast as a research fellow. Between 2002 and 2018, he was a Lecturer (2002), a Senior Lecturer (2007), a Reader (2009) and a Chair Professor (2011) with the School of Electronics, Electrical Engineering and Computer Science, Queen's University Belfast, Belfast, U.K. He currently holds the Chair of Smart Energy Systems at the University of Leeds, UK. His research interests cover nonlinear system modelling, identification, and control, and machine learning, with substantial applications to energy and power systems, smart grid, transport decarbonization, and energy management in energy intensive manufacturing processes.